TURNOVER RATE OF SOIL ORGANIC MATTER AND ORIGIN OF SOIL $^{14}CO_2$ IN DEEP SOIL FROM A SUBTROPICAL FOREST IN DINGHUSHAN BIOSPHERE RESERVE, SOUTH CHINA

P Ding[1,2] • C D Shen[1,3] • N Wang[1] • W X Yi[1] • X F Ding[3] • D P Fu[3] • K X Liu[3] • L P Zhou[4]

ABSTRACT. This paper examines the carbon isotopes (^{13}C, ^{14}C) of soil organic carbon (SOC) and soil CO_2 from an evergreen broadleaf forest in southern China during the rainy season. The distribution of SOC $\delta^{13}C$, and SOC content with depth, exhibits a regular decomposition of SOC compartments with different turnover rates. Labile carbon is the main component in the topsoil (0–12 cm) and has a turnover rate between 0.1 and 0.01 yr^{-1}. In the middle section (12–35 cm), SOC was mainly comprised of mediate carbon with turnover rates ranging between 0.01 and 0.025. Below 35 cm depth (underlayer section), the SOC turnover rate is slower than 0.001 yr^{-1}, indicating that passive carbon is the main component of SOC in this section. The total production of humus-derived CO_2 is 123.84 g C m^{-2} yr^{-1}, from which 88% originated in the topsoil. The middle and underlayer sections contribute only 10% and 2% to the total humus-derived CO_2 production, respectively. Soil CO_2 $\delta^{13}C$ varies from −24.7‰ to −24.0‰, showing a slight isotopic depth gradient. Similar to soil CO_2 $\delta^{13}C$, $\Delta^{14}C$ values, which range from 100.0‰ to 107.2‰, are obviously higher than that of atmospheric CO_2 (60–70‰) and SOC in the middle and underlayer section, suggesting that soil CO_2 in the profile most likely originates mainly from SOC decomposition in the topsoil. A model of soil CO_2 $\Delta^{14}C$ indicates that the humus-derived CO_2 from the topsoil contributes about 65–78% to soil CO_2 in each soil gas sampling layer. In addition, the humus-derived CO_2 contributes ~81% on average to total soil CO_2 in the profile, in good agreement with the field observation. The distribution and origin of soil $^{14}CO_2$ imply that soil CO_2 will be an important source of atmospheric $^{14}CO_2$ well into the future.

INTRODUCTION

Soil organic carbon (SOC) contains about 127 × 10^{15} g C (Sombroek et al. 1993), contributing nearly 61.7 Pg C per year, ~10% of the total carbon of atmospheric CO_2 (760 Pg C), to the atmosphere (Schimel 1995; IPCC 2000). With respect to global change, whether SOC is playing a source or sink for atmospheric CO_2 remains unknown. This partly depends on the variation of SOC turnover rate under the increasing atmospheric temperature that would speed up the soil respiration rate (Kirschbaum 1995; Goulden et al. 1998). Since forest ecosystems in tropical and subtropical areas contain ~37.3% of the total organic carbon in all forest ecosystems, and almost half is stored in soils (WBGU 1998), it is crucial to identify the vertical distribution patterns and turnover rates of SOC. Sources of SOC are mainly controlled by vegetation types and topography (Kuzyakov and Domanski 2000; Bird et al. 2001). SOC has a similar isotopic composition to that of source plants (Flanagan et al. 1999; Lin et al. 1999). For a certain profile with continuous coverage of the same plant, the variation of SOC $\delta^{13}C$ along depth is attributed to isotopic fractionation during the SOC decomposition process. Therefore, SOC $\delta^{13}C$ values correlate well with soil organic matter (SOM) sources, SOC composition, and turnover processes during soil development (Chen et al. 2005). With respect to SOC turnover rates, bomb ^{14}C is a unique tracer to evaluate the rate (Levin and Hesshaimer 2000). Cherkinsky and Brovkin (1993) presented a simple model to calculate turnover rates of SOC, which has been further developed to calculate the production of humus-derived soil CO_2 by Chen et al. (2002b) and Tao et al. (2007). Soil CO_2 is produced through biological process including organic matter decomposition and root respiration, then it transports to the overlying atmosphere via molec-

[1]Key Laboratory of Isotope Geochronology and Geochemistry, Guangzhou Institute of Geochemistry, Chinese Academy of Sciences, Guangzhou 510640, China.
[2]Corresponding author. Email: cdshen@gig.ac.cn.
[3]State Key Laboratory of Nuclear Physics and Technology, Peking University, Beijing 100871, China.
[4]Laboratory for Earth Surface Processes, Department of Geography, Peking University, Beijing 100871, China.

Proceedings of the 20th International Radiocarbon Conference, edited by A J T Jull
RADIOCARBON, Vol 52, Nr 2–3, 2010, p 1422–1434

ular diffusion (Amundson et al. 1998). It is therefore crucial to determine the contribution of humus-derived CO_2 to soil CO_2 for determining whether SOC is a source or sink for the atmospheric CO_2.

The selected monsoon evergreen broad-leaf forest in the Dingshuan Biosphere Reserve (DBR) has been well documented (Yu and Peng 1995; Shen et al. 1999; Chen et al. 2005; Yi et al. 2006). Recent research showed that the forest ecosystem is a possible sink for atmospheric CO_2 due to the continuous accumulation of SOC (Zhou et al. 2006). Further work has been taken to partition the contribution of SOC decomposition and root respiration to soil CO_2 in the forest. Yi et al. (2007) suggested that SOC decomposition was the main source of soil CO_2 in the rainy season. Although we have known the total amount of the humus-derived CO_2 in soil respiration for a short period by field observation, the total production of humus-derived CO_2 and the contribution from each layer corresponding to different decomposition stages and composition of SOC remained unknown. In order to clarify the questions above, we have collected soil samples and soil CO_2 samples from the soil profile Dinghu Lingshi (DHLS) in DBR.

In this paper, we calculate the turnover rates of SOC and evaluate the humus-derived CO_2 production in each sampling layer. We also compare the ^{14}C content of SOC and soil CO_2, and discuss the origin of soil CO_2 in deep soil layers.

Location of the Study Site

The Dingshuan Biosphere Reserve (DBR) (23°9′–23°11′N, 112°30–112°33′E) is located in northeast Zhaoqin, Guangdong Province (Figure 1), and has a southern, subtropical-monsoon humid climate. The average annual temperature is 21.8 °C, and the mean annual rainfall is 1927 mm in the study area. April through September is the rainy season with a mean monthly rainfall of 200 mm, and November to January is the dry season with mean monthly rainfall of 22–50 mm (Deng et al. 1990; Yu and Peng 1995). The pine forest, pine and broadleaf mixed forest, and monsoon evergreen broadleaf forest show the natural evolution sequence of vegetation along the elevation from 1000 to 14 m in DBR. Tropical monsoon rainy forest and subtropical monsoon evergreen broadleaf forest are the typical forest ecosystems in southern China (Tu 1984; Yi et al. 2007).

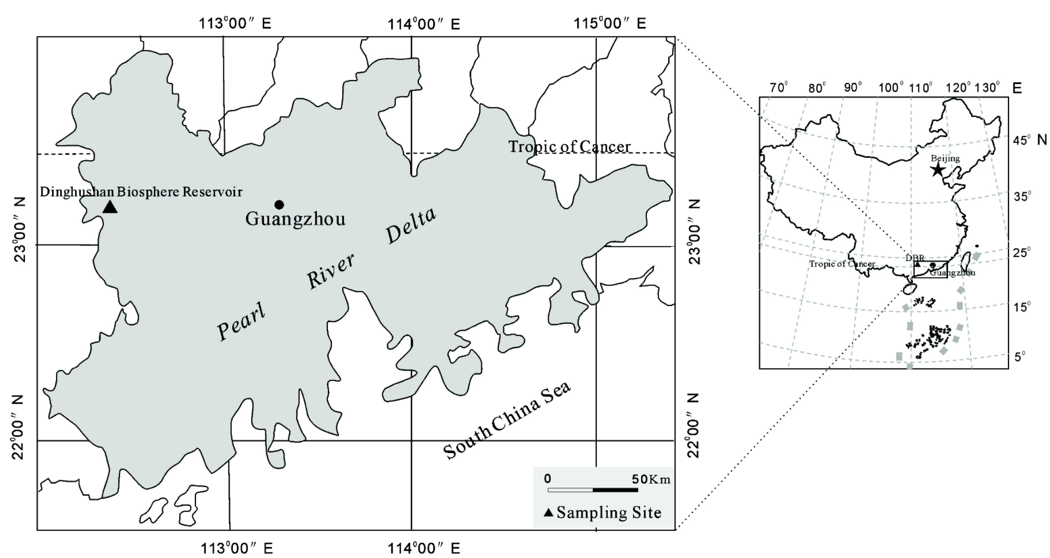

Figure 1 Location of Dinghushan Biosphere Reservoir and the sampling profile

https://doi.org/10.1017/S0033822200046506 Published online by Cambridge University Press

METHODS

Collection of Soils and Soil Gas Samples

In our study, we selected a natural, undisturbed soil profile (DHLS) in the monsoon evergreen broadleaf forest in DBR from which we collected our soil and soil CO_2 samples in July 2007. This was during the rainy season when microbial activity and root respiration are active. The main plant community comprises *Castanopsis chinensis*, *Schima superba*, and *Cryptocarya* spp. Lateritic red earth is the soil type of the forest. A detailed description of the soil profile is given in Table 1.

Table 1 Description of the soil profile Dinghu Lingshi (DHLS) (23°10′16″ N, 112°32′23″E), elevation 260 m, slope ~30°.

Depth (cm)	Description
0~20	Putrid litter at 0 cm; loose, humid, gray colored; enriched in roots and organic carbon
20~35	Moisture, brownish gray, containing less roots
35~70	Moisture, compact, yellowish brown, with few roots
70~90	Moisture, compact, yellow colored, rare roots, increased weathered clastic rock

Soil samples were collected at different intervals corresponding to the different soil layers. From the top to 30 cm depth, corresponding to the litter layer and humic layer (O+A+AB), the soil was sampled in 2-cm layers using the method proposed by Becker-Heidmann et al. (1996). In these 2 layers, the total organic carbon (TOC) usually accounts for more than 90% of the whole profile (Chen et al. 2002a). The soil was then sampled in 5-cm intervals from 30 to 50 cm depth and in 10-cm intervals from 50 to 90 cm depth, corresponding to layers B and B+BC, respectively. Soil gas was collected at 15-cm intervals down to 90 cm. Before the soil gas collection, we vacuumed sampling bags with 500 mL in volume under 10^{-3} Torr conditions and ensured the bags could remain at 10^{-2} Torr without vacuuming for at least 8 hr. When we extracted the soil gas, we first inserted a stainless steel tube with an inner diameter of 1 mm into the soil profile about 50 cm horizontally, then extracted the soil gas at a rate of 4 times per minute using a hand vacuum pump (Mityvac) with 16 mL in volume. To avoid contamination from atmospheric CO_2 previously existing in the pipe, we discharged the gas at first for half a minute, then extracted and collected the soil gas into vacuumed sampling bags. Previous observation has shown that the flux of soil CO_2 was 477.9 ± 96.3 mg hr^{-1} m^{-2}, ~1.75–2.62 mg C min^{-1} m^{-2} (Yi et al. 2007), and the soil CO_2 concentration varied between 6000–16,000 ppmv in the rainy season (Yi et al. 2006). Therefore, under stable conditions of soil CO_2, each layer (6 sampling layers in each profile) would derive 0.30–0.46 mg C min^{-1} m^{-2} higher than our extraction rate 0.10~0.28 mg C min^{-1}. This ensured the soil CO_2 would not mix with other layers when we pumped the soil gas. In order to get enough C (0.5–1.0 mg) for analysis, it took about 5 min in the upper layer and 4 min in the under layer for soil gas sampling.

Sample Preparation

Soil samples were first dried by a vacuum freeze drier. After removing visible roots and stone fragments, about 3–5 g of soil subsamples were treated with 2M HCl to eliminate cohesive carbonate, then rinsed with distilled water. After being dried at 70 °C in an oven, the subsamples were ground and mixed well. Sufficient soil samples were then placed into quartz tubes with silver wire and clean, grainy CuO. After the tubes were vacuumed and sealed, subsamples were combusted at 850 °C in a muffle furnace for 2 hr to transform the SOC into CO_2. Burned tubes were cracked open in the tube cracker and the gas was released from the samples. The soil CO_2 was then purified using liquid N_2 and liquid N_2+ethanol traps in the vacuum system, and was quantified by measuring the

CO_2 pressure with a microbarograph. The purified CO_2 was divided into 2 portions with 1 portion containing 0.5–1.0 mg C for the graphite target preparation using the method proposed by Xu et al. (2007). The other portion was frozen in a vacuum tube and sealed by torch for stable carbon isotope analysis. The soil CO_2 content was measured using an AGILENT-6890N gas chromatograph in the State Key Laboratory of Organic Geochemistry, Chinese Academy of Sciences (CAS), soon after gas samples were sent back to the laboratory. Purification of soil CO_2 from the residual soil gas and graphite preparation were done in the same way.

Pretreatment and graphite preparation of SOC and soil CO_2 were carried out at the accelerator mass spectrometry (AMS) ^{14}C laboratory in the Key Laboratory of Isotope Geochronology and Geochemistry, CAS. The graphite targets were measured at the Key Laboratory of Nuclear Physics and Technology (Peking University) AMS facility with a precision better than 0.5%. $\delta^{13}C$ values of the purified CO_2 gas were analyzed using a Finnigan MAT-251 mass spectrometer with a precision of ±0.2 in the State Key Laboratory of Loess and Quaternary Geology (Xi'an, China). Results are reported as $\delta^{13}C$ with the international Pee Dee belemnite (PDB) standard.

RESULTS AND DISCUSSION

Vertical Distribution of SOC $\delta^{13}C$ and SOC Content

SOC $\delta^{13}C$ is typically lowest at the surface and increases with depth until reaching the maximal value at 0.4 m (Figure 2). It ranges from –29.0‰ to –22.3‰, a variation of about 6.7‰. Meanwhile, SOC content decreases exponentially with increasing depth from the maximal value 4.6% at the surface to 0.4% in the bottom and trends towards a stable value (Figure 2). Sources of SOC are mainly controlled by vegetation and topography, and SOC $\delta^{13}C$ values are associated with SOC sources, decomposition, and turnover process during soil development (Bird et al. 2001; Chen et al. 2005). With continuous coverage of the same plant type, the vertical variation of SOC $\delta^{13}C$ is attributed to isotopic fractionation during SOC decomposition (Schweizer et al. 1999; Hobbie et al. 2004). For modeling purposes, SOC can be divided into 3 components of different turnover time: active carbon (<1 yr), labile carbon (1–100 yr), and passive carbon (>100 yr) (Trumbore and Gaudinsky 2003). Active carbon usually decomposes within 10 yr, with $\delta^{13}C$ increasing rapidly due to carbon isotope fractionation (Figure 2). Then, the labile carbon decomposes, resulting in the further enrichment of ^{13}C and the greatest $\delta^{13}C$ value generally, which indicates that most of the SOC has decomposed and the remaining SOC is mainly passive carbon with higher $\delta^{13}C$. The turnover rate of SOC then slows down, and the SOC content reduces slightly and tends to be stable along depth. When the passive carbon has decomposed, the SOC gradually becomes depleted in ^{13}C, probably due to the decomposition of SOC compartments with high $\delta^{13}C$ value, which thus led to the decrease of SOC $\delta^{13}C$ with increasing depth (Chen et al. 2005).

^{14}C Dating of SOC

^{14}C content is reported as $\Delta^{14}C = (A_{SN}/A_{ABS}-1) \times 1000‰$. As shown in Table 2, SOC in the 0–35 cm section is mainly composed of litter and humic substances with modern carbon affected by atmospheric nuclear tests ($\Delta^{14}C$ ranging from 25.8‰ to 140.8‰). The maximal depth "bomb ^{14}C" reaches is usually called the penetrating depth of bomb ^{14}C (Shen et al. 1999). In DHLS, the penetrating depth of bomb ^{14}C is 35 cm, close to the depth showing the maximal value of $\delta^{13}C$ (40 cm).

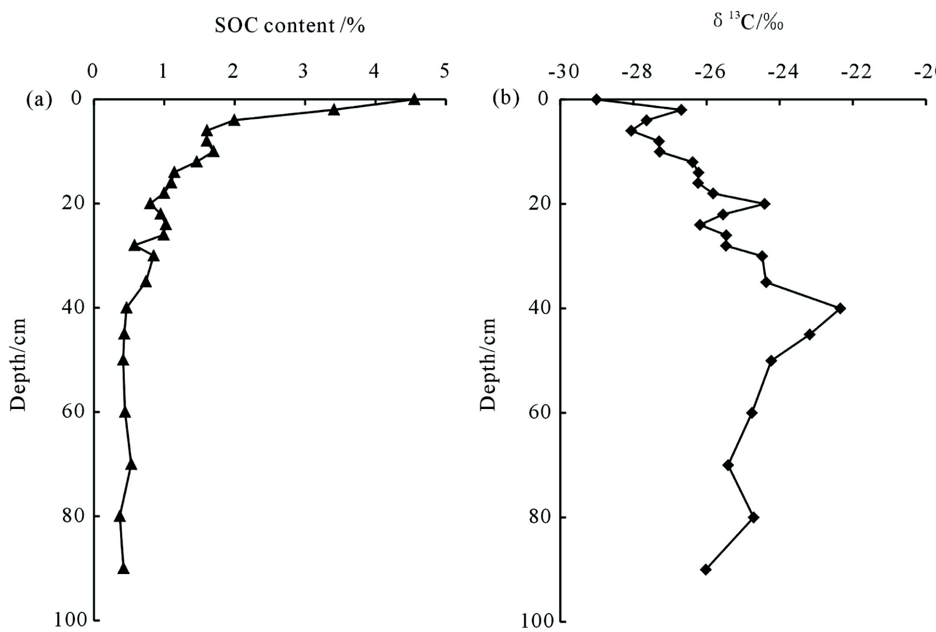

Figure 2 Variation of SOC content and SOC $\delta^{13}C$ with depth

Table 2 Carbon isotopic compositions and the calculated turnover rate of SOC in each sampling layer in DHLS, as well as the calculated the flux of soil CO_2 derived from SOC decomposition.

Lab code	Field code (DLHS-)	Depth (cm)	TOC (%)	$\delta^{13}C$ (‰)	PMC (%)	Error (‰)	PMC (calib-rated)	$\Delta^{14}C$ (‰)	Decom-position rate (yr^{-1})	Flux (g C $cm^{-2}\,yr^{-1}$)	Contri-bution	Accum-ulation (%)
GZ1807	S00	0	4.55	−29.01	109.49	0.43	110.37	103.7	0.102620	0.003035	0.245102	24.51
GZ1808	S01	2	3.41	−26.69	114.55	0.39	114.94	149.4	0.053940	0.004782	0.386123	63.12
GZ1809	S02	4	1.99	−27.64	112.71	0.4	113.31	133.1	0.018180	0.000942	0.076055	70.73
GZ1810	S03	6	1.60	−28.06	111.89	0.41	112.57	125.7	0.016360	0.000682	0.055104	76.24
GZ1811	S04	8	1.60	−27.3	110.26	0.4	110.77	107.7	0.012940	0.000539	0.043499	80.59
GZ1812	S05	10	1.70	−27.28	109.92	0.36	110.42	104.2	0.012380	0.000547	0.044167	85.00
GZ1813	S06	12	1.46	−26.38	108.97	0.36	109.27	92.7	0.010720	0.000407	0.032855	88.29
GZ1814	S07	14	1.14	−26.22	105.7	0.36	105.96	59.6	0.007040	0.000209	0.016877	89.98
GZ1815	S08	16	1.10	−26.23	103.95	0.37	104.21	42.1	0.005600	0.000160	0.012898	91.27
GZ1816	S09	18	1.00	−28.5	101.91	0.36	102.62	26.2	0.004500	0.000117	0.009410	92.21
GZ1817	S10	20	0.80	−24.41	95.58	0.49	95.47	−45.3	0.002622	0.000055	0.004401	92.65
GZ1818	S11	22	0.95	−25.55	101.87	0.36	101.98	19.8	0.004100	0.000101	0.008153	93.46
GZ1819	S12	24	1.02	−26.18	105.36	0.35	105.61	56.1	0.006720	0.000178	0.014403	94.90
GZ1820	S13	26	0.99	−25.46	102.24	0.39	102.33	23.3	0.004320	0.000111	0.008978	95.80
GZ1821	S14	28	0.58	−25.47	102.7	0.4	102.80	28.0	0.004600	0.000069	0.005571	96.36
GZ1822	S15	30	0.85	−24.48	99.99	0.4	99.89	−1.1	0.003210	0.000071	0.005716	96.93
GZ1823	S16	35	0.74	−24.37	100.05	0.34	99.92	−0.8	0.003140	0.000151	0.012174	98.15
GZ1824	S17	40	0.46	−22.34	84.31	0.34	83.86	−161.4	0.000647	0.000020	0.001575	98.31
GZ1825	S18	45	0.43	−23.18	85.09	0.34	84.78	−152.2	0.000693	0.000019	0.001570	98.46
GZ1826	S19	50	0.42	−24.23	84.71	0.31	84.58	−154.2	0.000683	0.000037	0.002976	98.76
GZ1827	S20	60	0.44	−24.76	83.7	0.34	83.66	−163.4	0.000637	0.000037	0.002960	99.06
GZ1828	S21	70	0.53	−25.41	88.67	0.38	88.74	−112.6	0.000981	0.000068	0.005460	99.60
GZ1829	S22	80	0.37	−24.71	74.29	0.32	74.25	−257.5	0.000359	0.000017	0.001383	99.74
GZ1830	S23	90	0.42	−26.02	82.33	0.49	82.50	−175.0	0.000587	0.000032	0.002590	100.00

Simulated SOC Turnover Rate and Soil CO_2 Production

Bomb ^{14}C in topsoil layers is now widely used to trace the turnover rate of SOC (Trumbore 1996; Chen et al. 2002b; Telles et al. 2003). In this paper, we applied the model presented by Cherkinsky and Brovkin (1993) to calculate the SOC turnover rate (m), and further the production of humus-derived CO_2 in each sampling layer. The equations used are as follows:

$$\frac{A_S(1955)}{A_{ABS}} = \frac{m}{m+\lambda} \tag{1}$$

$$A_S(t) = A_S(t-1) - (m+\lambda) \cdot A_S(t-1) + m \cdot A_0(t) \tag{2}$$

where $A_S(1955)$ is the SOC ^{14}C specific activity in 1955, $A_S(t)$ is the ^{14}C-specific activity of SOC in the sampling year ($t > 1955$), $A_S(t-1)$ is ^{14}C-specific activity of SOC in years ($t-1$), $A_0(t)$ is the atmospheric ^{14}C-specific activity in year t, A_{ABS} is the absolute international standard activity (equal to 0.95 times the ^{14}C activity of OXI normalized to $\delta^{13}C = -19‰$ and the year 1950; Stuiver and Polach 1977), λ is the ^{14}C decay constant (1/8033 yr^{-1}), and m is the SOC turnover rate (yr^{-1}).

Equation 1 represents the variation of SOC ^{14}C-specific activity in a stable and closed soil section. Equation 2 describes the SOC ^{14}C-specific activity in an open soil section that is exchanging with atmospheric CO_2. The mathematical expression means that the ^{14}C-specific activity of SOC in year t is determined by the ^{14}C-specific activity in the year (t–1), the loss of ^{14}C by natural decay and SOC decomposition in the year (t–1), and the incorporation of new ^{14}C-specific activity from the atmosphere through new formation of organic matter in the year t. According to the definition of percent modern carbon (pMC), the ^{14}C-specific activity could be expressed below in pMC.

$$pMC = \left(\frac{A_{SN}}{A_{ABS}}\right) \times 100\% \tag{3}$$

$$pMC_S(1955) = \frac{m}{m+\lambda} \tag{4}$$

$$pMC_S(t) = pMC_S(t-1) - (m+\lambda)pMC_S(t-1) + m pMC_0(t) \tag{5}$$

where pMC_S and pMC_0 represent the percent modern carbon of SOC and the atmosphere, respectively. Before the simulation, measured pMC values of SOC were corrected by normalizing SOC $\delta^{13}C$ values to −25‰:

$$A_{SN} = A_S\left(1 - \frac{2 \times (25 + \delta^{13}C)}{1000}\right) \tag{6}$$

We compiled a computer program to calculate m. First, assume $m = 0$, and then I (1955) is calculated by Equation 4. The values of I (1955) and m are then put into Equation 5, and the pMC_S (2007) is obtained by iterative calculation. Change m with an increase of 0.00002 each time and repeat the process above until the calculated pMC_S (2007) is the closest to the measured pMC_S (2007). Then, m is the result that we wanted. When 2 possible m values are suggested (Townsend et al. 1995), one is selected by considering m values of adjacent layers. Values of $pMC_0(t)$ in 1955–1958, 1959–2003, and 2004–2007 were obtained from Hua and Barbetti (2004), Levin and Kromer (2004), and results calculated from the equation proposed by Levin and Kromer (1997), respectively.

In the soil section with SOC $\Delta^{14}C < 0$, the SOC is considered to be stable and has not been influenced by bomb ^{14}C. According to Equation 1 and the definition of $\Delta^{14}C$, the turnover rate (m) of SOC could be calculated as Trumbore (1996):

$$m = -\lambda\left(\frac{1000}{\Delta^{14}C} + 1\right) \tag{7}$$

Since SOC decomposes and is lost mainly as soil CO_2, the production of humus-derived CO_2 in each sampling layer could be computed as:

$$P_i = \rho \times h_i \times C_i \times m_i \tag{8}$$

where P_i denotes humus-derived CO_2 production, h_i is the thickness, C_i is the SOC content, m_i is the turnover rate in the sampling layer i, and ρ represents the bulk density of soil and equals 1.3 g cm^{-3} in our calculation (Yi et al. 2006). The thickness of the surface soil layer is assumed to be 0.5 cm. Calculated results are shown in Table 2.

The total production of humus-derived CO_2 in the soil profile is 123.84 g C m^{-2} yr^{-1} (~518.37 mg CO_2 m^{-2} hr^{-1}). Field observations (Yi et al. 2007) show that SOC decomposition contributes ~400 mg CO_2 m^{-2} hr^{-1} to soil CO_2 flux in the rainy season, i.e. ~80% of the production of humus-derived CO_2 in the profile. Our calculation does not consider partly formed humic acid and microbial biomass, which may explain the lower measured values. Some 88% of the humus-derived CO_2 originates in the topsoil layers (above 12 cm) (see Figure 3).

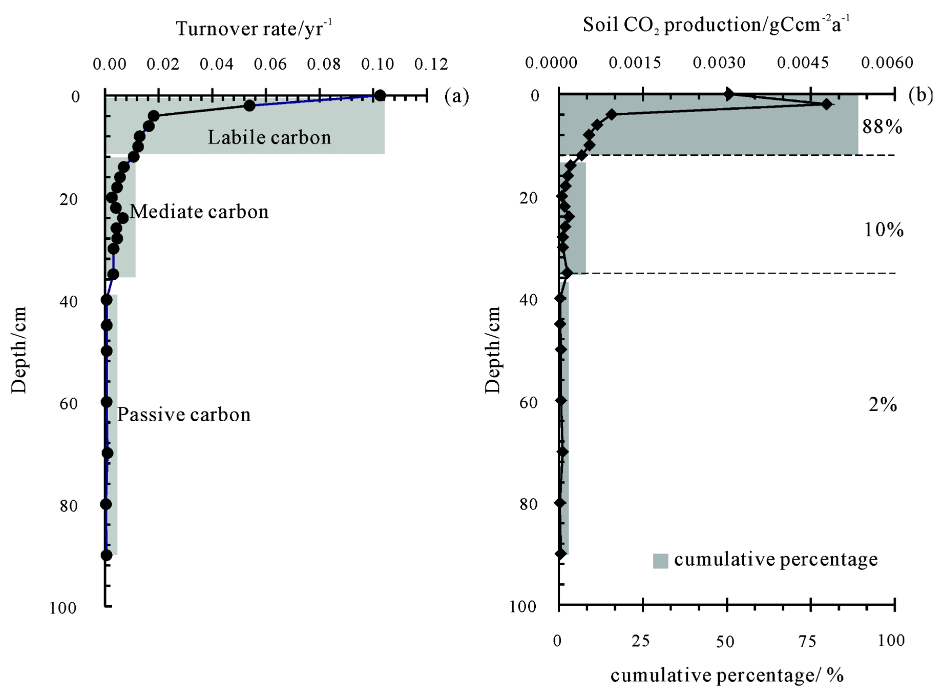

Figure 3 Turnover rates of SOC and the production of humus-derived soil CO_2 versus depth. (a) SOC turnovers at different rates corresponding to the different components of carbon with depth. (b) About 88% of humus-derived CO_2 originates from the topsoil layers and decomposing labile carbon, while the mediate carbon and passive carbon related with the middle and under soil section contributes only 10% and 2% to total production of humus-derived CO_2, respectively.

https://doi.org/10.1017/S0033822200046506 Published online by Cambridge University Press

In the topsoil, SOC turnover rates are between 0.1 and 0.01 yr^{-1}, indicating that SOC is mainly composed of labile carbon. In the middle part of the soil profile, from 12 to 35 cm, SOC turnover rates lie within 100 and 400 yr, contributing ~10% of the total humus-derived CO_2 production. According to the SOC turnover rate, SOC in this soil section is primarily composed of passive carbon; however, the turnover rate is closer to that of labile carbon. Thus, we call it "mediate carbon," between labile and passive carbon. Passive carbon is the main component of SOC in the deeper part of the soil, from 40 to 90 cm. It turns over at a relatively slow rate, longer than 1000 yr, and contributes only about 2% of total humus-derived CO_2 production.

Carbon Isotopic Composition of Soil CO_2

The $\delta^{13}C$ of soil CO_2 is expected to decrease from the atmospheric value near the surface to a value approaching that of the decomposing SOC or root respiration (plus a minimum 4.4‰) with increasing depth due to the decline in the incorporation of atmospheric CO_2 (Amundson and Davidson 1990). However, in the DHLS profile, soil CO_2 $\delta^{13}C$ ranges from −24.7‰ to −24.0‰ (Table 3), almost constantly throughout, which means the influence of atmospheric CO_2 is negligible here. When SOC decomposes and roots respire, the ^{13}C fractionation is be insignificant and is considered to have the same $\delta^{13}C$ values as origin substrates (Enting et al. 1995; Robinson and Scrimgeour 1995; Flanagan et al. 1999; Lin et al. 1999). Since the profile covered the same plant type, the soil CO_2 derived from root respiration should have similar $\delta^{13}C$ values along the depth. However, SOC decomposition, as shown in Figure 2, will contribute varying $\delta^{13}C$ values of soil CO_2.

Table 3 $\delta^{13}C$ and $\Delta^{14}C$ content of soil CO_2 in the DHLS profile.

Depth (cm)	Content (ppmv)	PMC (%)	$\delta^{13}C$ (‰)	$\Delta^{14}C$ (‰)
15	10072	110.17	–24.34	101.7
30	9539	110.18	–24.16	101.8
45	14086	110.72	–24.49	107.2
60	10411	110.63	–24.41	106.3
75	18718	110.51	–24.71	105.1
90	6120	110.00	–24.03	100.0

Theoretically, the $\delta^{13}C$ distribution of soil CO_2 would reflect a measurable isotopic gradient with depth, and the variation would depend on the ratio of humus-derived CO_2 to total soil CO_2. The actual situation is more complicated. Two possible scenarios could lead to the $\delta^{13}C$ distribution of soil CO_2, and they differ from the ideal condition. One links to the ratio of soil CO_2 derived from SOC decomposition to total soil CO_2. If SOC decomposition contributes little, while most of soil CO_2 originates from root respiration, the soil CO_2 $\delta^{13}C$ would be closer to that of roots and thus inclined to have similar values. The other scenario is related to the diffusion of soil CO_2. Previous observation proposed that the measurable isotopic gradients of soil CO_2 $\delta^{13}C$ are more obvious in soils that respire at lower rates (Amundson et al. 1998). This means that if the soil in DHLS respires at a high rate, the diffusion of soil $^{13}CO_2$ would lead to the soil $^{13}CO_2$ distributing equally with depth because of the correspondingly fast diffusion rate. In order to clarify which of these scenarios is the real cause, it is important to understand the origin of the soil CO_2.

Bomb ^{14}C provides us not only with a method to calculate the turnover rate of SOC, but also a tracer to identify the soil CO_2 sources. Isotopic fractionations during fixation or root respiration can be neglected, according to Trumbore (2000). ^{14}C values of soil CO_2 derived from SOC decomposition and root respiration are therefore close to those of SOC and roots. Since the roots involved in respiration are currently produced, $\Delta^{14}C$ values of soil CO_2 derived from root respiration are identical to that of atmospheric CO_2 (Wang et al. 1994; Hobbie et al. 2002; Liu et al. 2006). Thus, similar to the theoretically expected distribution of $\delta^{13}C$, soil CO_2 $\Delta^{14}C$ would also exhibit an isotopic gradient along depth with values ranging between those of current atmospheric CO_2 and SOC in the same soil layer. Since $\Delta^{14}C$ of atmospheric CO_2 reached a peak of ~900‰ in 1964, it decreased sharply to 60–70‰ at present (Levin and Kromer 2004). As shown in Figure 4, $\Delta^{14}C$ values of soil CO_2 range between 100.0‰ to 107.2‰ in DHLS, showing no significant variation along depth and are obviously higher than that of SOC in the same layer and atmospheric CO_2 by 30‰ at least.

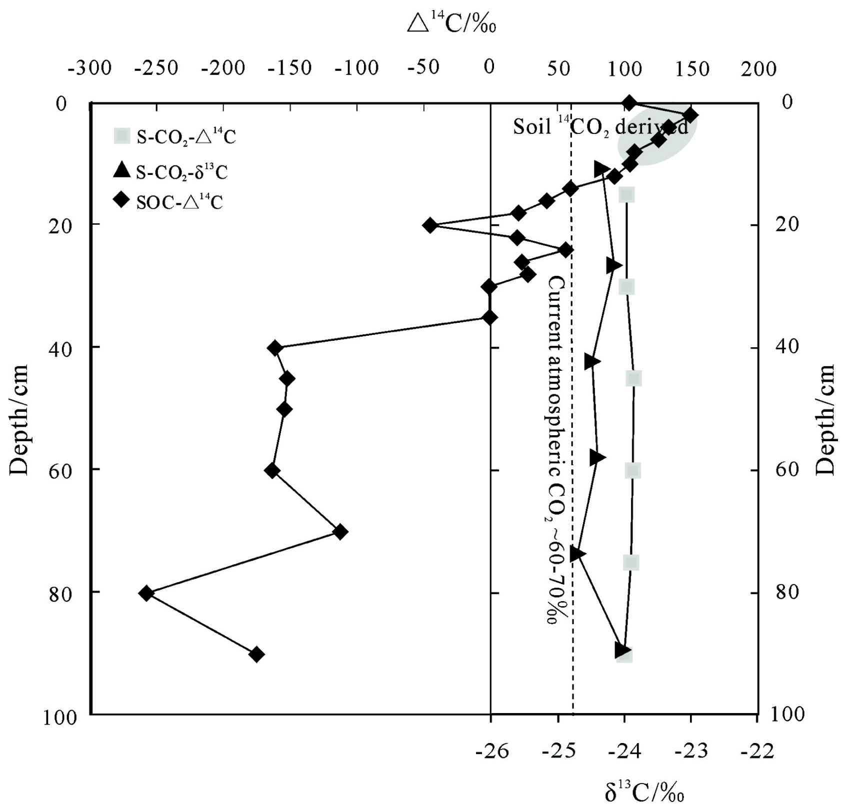

Figure 4 Distribution of $\Delta^{14}C$ values of SOC and soil CO_2 with depth in DHLS, as well as soil CO_2 $\delta^{13}C$ values. The shaded area (topsoil) represents main layers from where the soil $^{14}CO_2$ was derived.

A possible cause of the soil CO_2 $\Delta^{14}C$ "enrichment" may be the fractionation along with soil $^{14}CO_2$ flux to the tropospheric CO_2. Since the diffusional enrichment of $\delta^{13}C$ is 4.4‰, the diffusional enrichment value of ^{14}C would be close to 8.8‰, which is clearly lower than the measured difference. A more reasonable explanation for such "enrichment" is the delayed decomposition of SOC formed during the peak time of bomb ^{14}C. This means that the soil $^{14}CO_2$ mostly derived from SOC decomposition in the topsoil, especially in the deeper place where the $\Delta^{14}C$ of SOC shifts to negative values (Figure 4). This is in good agreement with the depth distribution of the origin of humus-derived CO_2, and can explain the soil CO_2 $\delta^{13}C$ distribution.

In order to evaluate the proportion of soil CO_2 derived from topsoil layers, we assumed the following: a) soil CO_2 derives from SOC decomposition in topsoil layers (0~12 cm) and root respiration; and b) root respiration contributes similar ^{14}C content to atmospheric CO_2 (~65‰).

https://doi.org/10.1017/S0033822200046506 Published online by Cambridge University Press

A 2 end-member mixing model could be expressed as follows:

$$\Delta^{14}C_{S-Aj} = \sum_{i=1}^{i=7} M_i C_i \times p_j + (1 - P_j) \times \Delta^{14}C_{atm}(i, j = 1, 2, 3\ldots\ldots) \tag{9}$$

where the $\Delta^{14}C_{S-Aj}$, M_i, C_i, P_j, and $\Delta^{14}C_{atm}$ denote, respectively, the $\Delta^{14}C$ value of soil CO_2 in the sampling layer *j*; $\Delta^{14}C$ value of SOC in the soil layer *i* in the topsoil; the relative percentage of the humus-derived CO_2 in layer *i*; the proportion of the humus-derived CO_2 from the topsoil in the layer *j*, and the $\Delta^{14}C$ value of atmospheric CO_2. Considering the influence of humus-derived CO_2 produced in deep soil layers, the calculation would be corrected as:

$$\Delta^{14}C_{S-Aj} = \sum_{i=1}^{i=24} M_i C_i \times F_j + (1 - F_j) \times \Delta^{14}C_{atm}(i, j = 1, 2, 3\ldots\ldots) \tag{10}$$

$$P_j = 0.88 \times F_j \tag{11}$$

where F_j represents the proportion of humus-derived CO_2 to total soil CO_2 in the layer *j*.

Results are depicted in Figure 5. Proportions of humus-derived CO_2 from the topsoil to total soil CO_2 calculated from the topsoil section and all depths range from 56% to 68% and 65% to 78%, respectively, which means that soil CO_2 is mainly derived from SOC decomposition in topsoil layers. Field observation has confirmed that the proportion of humus-derived (including rhizomicrobial respiration and root-free soil microbial respiration) CO_2 to soil respiration is ~80% during this time of year (Yi et al. 2007). In our simulation, F_j ranges from 74% to 89% with an average value of 81%, in agreement with the field observation.

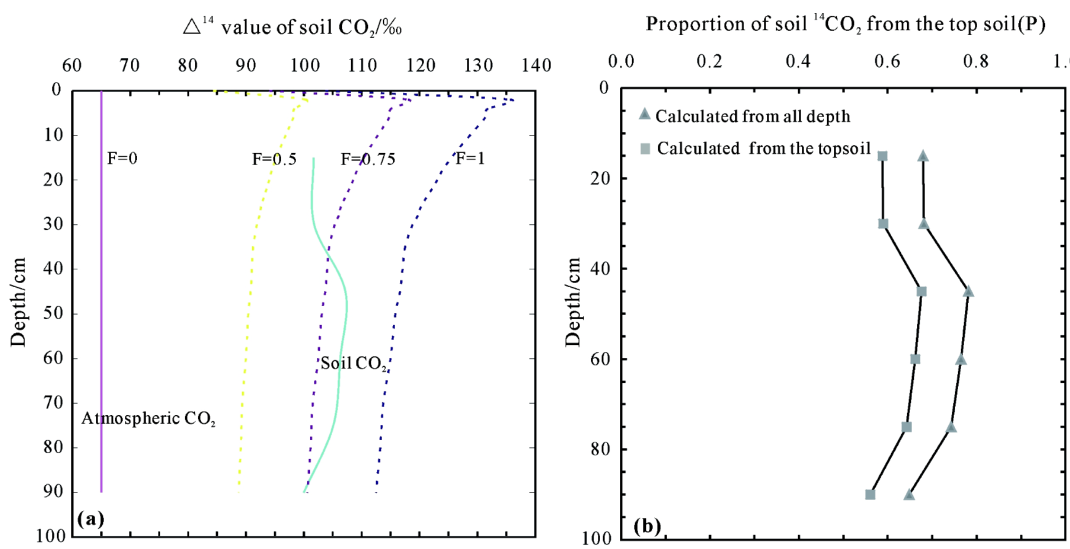

Figure 5 a) Modeled $\Delta^{14}C$ values of soil CO_2 for different depths and proportions of humus-derived CO_2 in DHLS, calculated from Equation 10 (see text). b) Proportion of soil $^{14}CO_2$ origins from the topsoil, calculated from the topsoil (assuming that the humus-derived CO_2 all originate from the topsoil layers) and all soil depth layers, respectively. The difference between the 2 methods is ~10% due to the incorporation of soil $^{14}CO_2$ originating from deeper SOC decomposition.

https://doi.org/10.1017/S0033822200046506 Published online by Cambridge University Press

Since soil CO_2 is mainly humus-derived from the topsoil, it is not difficult to understand why the terrestrial biosphere is currently releasing relatively ^{14}C-enriched CO_2 to the troposphere, especially in the boreal forest where SOC decomposes at a low rate (Randerson et al. 2002). One of the remaining questions is how the ^{14}C-enriched CO_2 enters the deep soil. Downward translocation of ^{14}C-enriched CO_2 can be responsible for most soil CO_2 in the deep soil layers. However, another possibility exists. Baisden and Parfitt (2007) found that the $\Delta^{14}C$ value had enriched over 200‰ in deep soil below 30 cm compared to a former investigation and suggested that dissolved organic carbon (DOC) with decadal turnover time was the primary contributor to the reactive SOC pool in deep soil layers. Fontaine et al. (2007) pointed out that the fresh carbon supply would stimulate microbial mineralization in deep soil layers. This means that soil CO_2 in deep soil layers may partly come from the decomposition of DOC that has moved to the deep soil. Further study should focus on the amount of dissolved carbon transmitted to the deep soil and to what extent the ^{14}C content changed in the deep soil layers.

SUMMARY AND CONCLUSION

The variation of SOC $\delta^{13}C$ and SOC content with depth showed a regular decomposition of SOC compartments with different turnover rates during soil development. SOC in topsoil (0–12 cm) is mainly composed of labile carbon with turnover rates ranging between 0.1 and 0.01 yr^{-1}. In the middle section of the soil profile (12–35 cm), the SOC was mainly comprised of mediate carbon with turnover rates ranging between 0.01 and 0.025. Under 35 cm depth, turnover rates of SOC decrease to slower than 0.001 yr^{-1} due to the main composition of passive carbon. During SOC decomposition, the total production of humus-derived CO_2 is 123.84 g C m^{-2} yr^{-1}. Production mainly originates from the topsoil, which contributes almost 88% to the total production of humus-derived CO_2. The middle section and underlayer contribute only 10% and 2%, respectively.

$\delta^{13}C$ of soil CO_2 varies from –24.7‰ to –24.0‰ and $\Delta^{14}C$ from 100.0‰ to 107.2‰ with a slight depth gradient. The $\Delta^{14}C$ value of soil CO_2 is obviously higher than that of atmospheric CO_2 (60–70‰) and SOC from the middle section and underlayer, suggesting that soil CO_2 in the profile is mainly derived from SOC decomposition from topsoil layers. The model concerning soil CO_2 $\Delta^{14}C$ indicates that the contribution of humus-derived CO_2 from the topsoil to soil CO_2 in each soil gas sampling layer ranges from 65% to 78%. In addition, the humus-derived CO_2 accounts for 74–89% to the total soil CO_2 in the profile with an average value of 81%. The distribution and origin of soil $^{14}CO_2$ imply that soil CO_2 will be an important source for atmospheric $^{14}CO_2$ well into the future.

ACKNOWLEDGMENTS

The authors are grateful to Dr Zou B at the South China Botanical Garden, Chinese Academy of Sciences (CAS), and Dr Fan AC in Hong Kong University for help with field sampling. This work was funded by the National Natural Science Foundation of China by grants 40231015 and 40473002, and by grants 2005CB422004 and KSCX2-SW-133 from the National Basic Research Program of China, and the Knowledge Innovation Program of the Chinese Academy of Sciences, respectively.

REFERENCES

Amundson RG, Davidson EA. 1990. Carbon dioxide and nitrogenous gases in the soil atmosphere. *Journal of Geochemical Exploration* 38(1–2):13–41.

Amundson R, Stern L, Baisden T, Wang Y. 1998. The isotopic composition of soil and soil-respired CO_2. *Geoderma* 82(1):83–114.

Baisden WT, Parfitt RL. 2007. Bomb ^{14}C enrichment indicates decadal C pool in deep soil? *Biogeochemistry* 85(1):59–68.

Becker-Heidmann P, Scharpenseel HW, Wiechmann H. 1996. Hamburg radiocarbon thin layer soils database. *Radiocarbon* 38(2):295–345.

https://doi.org/10.1017/S0033822200046506 Published online by Cambridge University Press

Bird MI, Lloyd J, Santruckova H, Veenendaal E. 2001. Global soil organic carbon. In: Schulze ED, Heimann M, Harrison S, Holland E, Lloyd J, Prentice IC, Schimel D, editors. *Global Biogeochemical Cycle in the Climate System*. New York: Academic Press. p 185–99.

Chen QQ, Shen CD, Peng SL, Sun YM, Yi WX, Li ZA, Jiang MT. 2002a. Soil organic matter turnover in the subtropical mountainous region of South China. *Soil Science* 167(6):401–15.

Chen QQ, Sun YM, Shen CD, Peng SL, Yi WX, Li ZA, Jiang MT. 2002b. Organic matter turnover rates and CO_2 flux from organic matter decomposition of mountain soil profiles in the subtropical area, south China. *Catena* 49(3):217–29.

Chen QQ, Shen CD, Sun YM, Peng SL, Yi WX. 2005. Spatial and temporal distribution of carbon isotopes in soil organic matter at the Dinghushan Biosphere Reserve, South China. *Plant and Soil* 273(1–2):115–28.

Cherkinsky AE, Brovkin VA. 1993. Dynamics of radiocarbon in soils. *Radiocarbon* 35(3):363–7.

Deng BQ, Lu LC, Wang DQ. 1990. The estimation of the microbial respiratory capacity and carbon balance of the soils in the forest ecosystem of Dinghushan Biosphere Reserve. *Tropical and Subtropical Forest Ecosystem* 6:41–6. In Chinese with English abstract.

Enting IG, Trudinger CM, Francey RJ. 1995. A synthesis inversion of the concentration and $\delta^{13}C$ of atmospheric CO_2. *Tellus B* 47:35–52.

Flanagan LB, Kubien DS, Ehleringer JR. 1999. Spatial and temporal variation in the carbon and oxygen stable isotope ratio of respired CO_2 in a boreal forest ecosystem. *Tellus B* 51:376–84.

Fontaine S, Barot S, Barr P, Bdioui N, Mary B, Rumpel C. 2007. Stability of organic carbon in deep soil layers controlled by fresh carbon supply. *Nature* 450(7167): 277–80.

Goulden ML, Wofsy SC, Harden JW, Trumbore SE, Crill PM, Gower ST, Fries T, Daube BC, Fan S, Sutton DJ, Bazzaz A, Munger JW. 1998. Sensitivity of boreal forest carbon balance to soil thaw. *Science* 279(5348): 214–7.

Hobbie EA, Tingey DT, Rygiewicz PT, Johnson MG, Olszyk DM. 2002. Contributions of current year photosynthate to fine roots estimated using a $\delta^{13}C$-depleted CO_2 source. *Plant and Soil* 247(2):233–42.

Hobbie EA, Johnson MG, Rygiewicz PT, Tingey DT, Olszyk DM. 2004. Isotopic estimates of new carbon inputs into litter and soils in a four-year climate change experiment with Douglas-fir. *Plant and Soil* 259(1–2):331–43.

Hua Q, Barbetti M. 2004. Review of tropospheric bomb ^{14}C data for carbon cycle modeling and age calibration purposes. *Radiocarbon* 46(3):1273–98.

IPCC (Intergovernmental Panel on Climate Change). 2000. *Land Use, Land Use Change, and Forestry.* Cambridge: Cambridge University Press.

Kirschbaum MUF. 1995. The temperature dependence of soil organic matter decomposition, and the effect of global warming on soil organic C storage. *Soil Biology and Biochemistry* 27(6):753–60.

Kuzyakov Y, Domanski G. 2000. Carbon input by plants into the soil. Review. *Journal of Plant Nutrition and Soil Science* 163(4):421–31.

Levin I, Hesshaimer V. 2000. Radiocarbon—a unique tracer of global carbon cycle dynamics. *Radiocarbon* 42(1):69–80.

Levin I, Kromer B. 1997. Twenty years of atmospheric $^{14}CO_2$ observations at Schauinsland station, Germany. *Radiocarbon* 39(2):205–18.

Levin I, Kromer B. 2004. The tropospheric $^{14}CO_2$ level in mid-latitudes of the Northern Hemisphere (1959–2003). *Radiocarbon* 46(3):1261–72.

Lin G, Ehleringer JR, Rygiewicz PT, Johnson MG, Tingey DT. 1999. Elevated CO_2 and temperature impacts on different components of soil CO_2 efflux in Douglas-fir terracosms. *Global Change Biology* 5(2):157–68.

Liu W, Moriizumi J, Yamazawa H. 2006. Depth profiles of radiocarbon and carbon isotopic compositions of organic matter and CO_2 in a forest soil. *Journal of Environment Radioactivity* 90(3):210–23.

Randerson JT, Enting IG, Schuur EAG, Caldeira K, Fung IY. 2002. Seasonal and latitudinal variability of troposphere $\Delta^{14}CO_2$: post bomb contributions from fossil fuels, oceans, the stratosphere, and the terrestrial biosphere. *Global Biogeochemical Cycles* 16(4):1112, doi:10.1029/2002GB001876.

Robinson D, Scrimgeour CM. 1995. The contribution of plant C to soil CO_2 measured using $\delta^{13}C$. *Soil Biology and Biochemistry* 27:1653–6.

Schimel DS. 1995. Terrestrial ecosystems and the carbon cycle. *Global Change Biology* 1:77–91.

Schweizer M, Fear J, Cadish G. 1999. Isotopic (^{13}C) fractionation during plant residue decomposition and its implications for soil organic matter studies. *Rapid Communications in Mass Spectrometry* 13(13):1284–90.

Shen CD, Liu TS, Peng SL, Sun YM, Jiang MT, Yi WX, Xing CP, Gao QZ, Li ZA, Zhou GY. 1999. ^{14}C measurement of forest soils in Dinghushan Biosphere Reserve. *Chinese Science Bulletin* 44(3):251–6.

Sombroek WG, Nachtergaele FO, Hebel A. 1993. Amounts, dynamics and sequestering of carbon in tropical and subtropical soils. *Ambio* 22:417–25.

Stuiver M, Polach HA. 1977. Discussion: reporting of ^{14}C data. *Radiocarbon* 19(3):355–65.

Tao Z, Shen CD, Gao QZ, Sun YM, Yi WX, Li YN. 2007. Soil organic carbon storage and soil flux in the alpine meadow ecosystem. *Science in China Series D* 50(7): 1103–14.

Telles EDC, Camargo PB, Martinelli LA, Trumbore SE, Costa ES, Santos J, Higuchi N, Oliverira Jr RC. 2003. Influence of soil texture on carbon dynamics and storage potential in tropical forest soils of Amazonia. *Glo-*

bal Biogeochemical Cycles 17(2):1040, doi:10.1029/2002GB001953.

Townsend AR, Vitousek PM, Trumbore SE. 1995. Soil organic matter dynamics along gradients in temperature and land use on the island of Hawaii. *Ecology* 76(3):721–33.

Trumbore SE. 1996. Applications of accelerator mass spectrometry to soil science. In: Boutton T, Yamasaki S, editors. *Mass Spectrometry of Soils*. New York: Marcel Dekker Inc. p 311–40.

Trumbore S. 2000. Age of soil organic matter and soil respiration: radiocarbon constraints on belowground C dynamics. *Ecological Applications* 10(2):399–41.

Trumbore SE, Gaudinsky JB. 2003. The secret lives of roots. *Science* 302(5649):1344–5.

Tu MZ. 1984. Litter production of evergreen broad-leaf forest in Dinghushan Biosphere Reserve. *Tropical and Subtropic Forest Ecosystem* 2:18–23. In Chinese with English abstract.

Wang Y, Amundson R, Trumbore S. 1994. A model for soil $^{14}CO_2$ and its implications for using ^{14}C to date pedogenic carbonate. *Geochimica et Cosmochimica Acta* 58(1):393–9.

WBGU (Wissenschaftlicher Beirat der Bundesregierung Globale Umweltvernderung). 1998. German Advisory Council on Global Change special report: the accounting of biological sinks and sources under the Kyoto Protocol. Bremerhaven, Germany.

Xu XM, Trumbore SE, Zheng SH, Southon JR, McDuffee KE, Luttgen M, Liu JC. 2007. Modifying a sealed tube zinc reduction method for preparation of AMS graphite targets: reducing background and attaining high precision. *Nuclear Instruments and Methods in Physics Research B* 259(1):320–9.

Yi ZG, Yi WM, Ding MM, Zhou LX, Zhang DQ, Wang XM. 2006. Vertical distribution of soil organic carbon soil microbial biomass and soil CO_2 concentration in Dinghushan Biosphere Reserve. *Ecology and Environment* 15(3):611–5. In Chinese with English abstract.

Yi ZG, Fu SL, Yi WM, Zhou GY, Mo JM, Zhang DQ, Ding MM, Wang XM, Zhou LX. 2007. Partitioning soil respiration of subtropical forests with different successional stages in south China. *Forest Ecology and Management* 243(2–3):178–86.

Yu ZY, Peng SL. 1995. The artificial and natural restoration of tropical and subtropical forests. *Acta Ecologica Sinica* 15(A):117. In Chinese with English abstract.

Zhou GY, Liu SG, Li ZA, Zhang DQ, Tang XL, Zhou CY, Yan JH, Mo JM. 2006. Old-growth forests can accumulate carbon in soils. *Science* 314(5804):1417.